AIAA JOURNAL
Vol. 46, No. 8, August 2008

Thermal Buckling and Postbuckling of Sandwich Panels with a Transversely Flexible Core

Yeoshua Frostig*
Technion–Israel Institute of Technology, 32000 Haifa, Israel
and
Ole Thybo Thomsen†
Aalborg University, 9220 Aalborg, Denmark

DOI: 10.2514/1.31704

This paper deals with thermally induced deformation buckling and postbuckling of a unidirectional sandwich panel with a soft core. The mathematical formulation is based on the high-order sandwich-panel approach and it incorporates the effects of the flexibility of the core in the vertical direction, along with its expansion or contraction in the vertical direction as a result of the imposed thermal field. The nonlinear governing equations are derived using a variational approach following the principles of the high-order sandwich-panel theory . The governing equations of the prebuckling and buckling states are determined through linearization following a perturbation approach. The effects of the vertical thermal core normal strains of the core, which are usually ignored by various computational models, are studied at the buckling and the postbuckling stages, with emphasis on the differences in the mechanical behavior. A comparison with results obtained using a classical elastic foundation approach is conducted, and the differences are presented and discussed. The postbuckling behavior of thermally loaded sandwich panels in the vicinity of the temperatures that cause buckling, based on a simplified model, is presented through numerical examples involving a uniform temperature field, along with finite element results using ANSYS that compare very well. In addition, the results for a gradient thermal field are described. The results are presented through various structural quantities along the panel and through equilibrium path curves of temperature vs extreme values of these structural quantities. An important conclusion of the study is that the postbuckling behavior of a heated sandwich panel with a soft core is of a stable type for the cases investigated (i.e., that of a plate rather than of a column or a shell).

Introduction

MODERN sandwich panels, which are made of a low-strength flexible core and two face sheets that are either made of metal or composite laminated materials, are widely used in the aerospace, naval, transportation, and building industry. They are used as primary and secondary structural components, and their popularity is a result of their superior qualities in terms of weight-to-strength ratio, high stiffness, ease of manufacturing, acoustic and thermal insulation, repair capability, and flexibility in design. During their service lifetime, such panels serve in various aggressive environments that exert induced deformation loads as a result of temperature changes, shrinkage, or moisture absorption. Thermally induced loads may be associated with bending, buckling, and postbuckling of such panels, and the goal of this research is to investigate the effect of thermally induced loads when large displacements are accounted for.

Thermal buckling (or thermally induced buckling) is defined by the critical temperature that causes loss of stability as a result of the development of in-plane compressive stress resultants that reach a critical value. In such a case, the critical temperature corresponds to the bifurcation point, the stage before the critical temperature is the prebuckling stage, and the stage of the critical temperature is the buckling stage. In general, these compressive stress resultants are a result of in-plane displacement constraints, especially when a uniform thermal field is considered (see Fig. 1). Notice that when such constraints do not exist, the sandwich panel undergoes deformations, with minor stress resultants that are mainly due to the mismatch of the expansion coefficients of the various constituents. The buckling phenomenon occurring in a unidirectional sandwich panel in the absence of imperfections is associated with a bifurcation load point that shifts from a membrane state, denoted as the prebuckling stage, into a bending state, denoted as the buckling stage, in which the in-plane compressive stress resultants remain nearly unchanged. In the case of a sandwich panel subjected to a uniform thermal field, the face sheets will undergo in-plane deformation, whereas the core undergoes vertical as well as in-plane displacements. If the upper-face sheet is not vertically supported, the vertical displacements of the core do not affect the deformation pattern of the face sheets at all, and the upper-face sheet will undergo a rigid-body movement (see Fig. 1a). However, when the upper-face sheet is restrained vertically at certain points (see Fig. 1b), the expansion/contraction of the core in the vertical direction causes bending and tensile or compressive stress resultants in the face sheets as a result of the in-plane restraints of the supports (immovable supports). Accordingly, the thermal buckling problem in a sandwich panel may be associated with a nonlinear behavior even at the very early stages of loading or prebuckling, rather than with a bifurcation point. A very important question, which is also one of the goals of this research, is how the vertical thermal displacements of the core affect the buckling and the postbuckling response of a sandwich panel.

The instability of sandwich panels with transversely rigid cores made of metallic or polymer honeycombs has been considered by many researchers. It is usually assumed that the core is of an antiplane type and incompressible (see, for example, the textbooks by Allen [1], Plantema [2], Zenkert [3], and Vinson [4]). In general, it is further assumed that the global and local (wrinkling) buckling modes of the sandwich panel are uncoupled (see also Bulson [5], Brush and Almroth [6], and Vinson and Sierakowski [7]). The global buckling

Received 19 April 2007; accepted for publication 15 April 2008.

*Professor of Structural Engineering, Ashtrom Engineering Company Chair in Civil Engineering, Faculty of Civil Engineering; cvrfros@techunix.technion.ac.il (Corresponding Author).

†Professor, Head of Institute, Institute of Mechanical Engineering, Pontoppidanstræde 101.

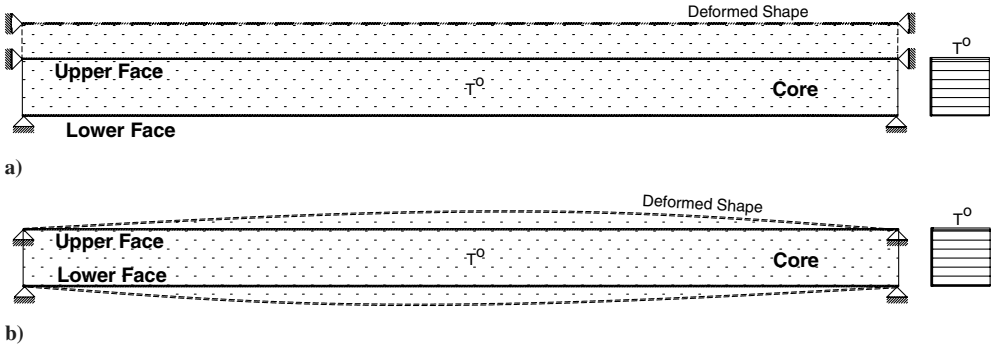

Fig. 1 Deformed shapes of uniformly heated sandwich panels: a) membranes state and b) nonmembrane state.

is defined through the solution of an equivalent panel that replaces the layered panel with an equivalent homogeneous layer (or equivalent single layer) that possess shear rigidity in addition to the flexural rigidity while ignoring the compressibility of the core. Among the commonly used theories for such analyses are the first-order shear deformation theory by Mindlin [8] or higher-order theories such as Reddy's [9]. In the case of thermal buckling and postbuckling of sandwich panels, various first- and high-order shear deformable models (along with analytical or finite element solutions that, in general, ignore the compressibility of the core) are proposed and used (see Ko [10], Kant and Babu [11], Najafizadeh and Heydari [12], Lanhe [13], Shiau and Kuo [14], and Matsunaga [15], who used truncated power series expansion of the distribution of the displacement patterns through the thickness), but are limited to simply supported boundary conditions and to buckling only. In general, the critical temperature at buckling is related to the compressive buckling stress resultants through the governing equations of the membrane state at the prebuckling stage, which ignores the expansion or contraction of the core under the thermal field. For local (wrinkling) buckling analysis, the sandwich panel is usually represented (idealized) by two isolated, separate, face sheets supported on an elastic foundation that is provided by the vertical rigidity of the core, while ignoring any interaction between the two face sheets, as well as through the shear and vertical normal stresses within the core (see, for example, Allen [1], Zankert [3], and Thomsen [16]). The same approach has also been applied for the case of thermal buckling (see Ko and Jackson [17]) and for intuitive/qualitative explanation of thermal postbuckling of a sandwich panel resting on an elastic foundation (see Rao and Raju [18]). Although the mechanical properties of the panel considered here are not affected by the thermal field, it is worthwhile to mention some recent works on the topic, for completeness. The effect of the temperature-dependent properties has been studied recently by Birman [19], who dealt with wrinkling of a simply supported sandwich panel using the first-order shear deformation model, along with material properties that linearly dependent on temperature. Recently, Birman et al. [20] and Liu et al. [21] considered the responses of a sandwich panel and a sandwich beam using the first-order shear deformation theory, with temperature-dependent properties and subjected to elevated temperatures.

A more rational approach models the layered sandwich panel as two face sheets and a core layer, which are combined/joined together through fulfillment of equilibrium and compatibility conditions, and thus is able to incorporate the vertical flexibility of the core, which has been ignored by many previously mentioned works. This approach has been implemented through a variational principle into the high-order sandwich-panel theory and has been used successfully for the analysis of various linear and nonlinear applications, including hygrothermal effects (see Frostig [22]), buckling analysis of unidirectional sandwich panels (see Frostig and Baruch [23]), buckling analysis of sandwich plates (see Frostig [24]), nonlinear response to in-plane compressive loads (see Sokolinsky and Frostig [25]), and a general nonlinear response (see Frostig et al. [26]).

The literature survey reveals that, in general, the proposed thermal buckling analyses of sandwich panels are limited to configurations with incompressible core materials (i.e., core materials that do not expand or contract when subjected to a thermal field, specific boundary conditions, and limiting assumptions. Hence, they are invalid/insufficient for the analysis of modern sandwich panels with compressible cores made of polymeric foam or low-strength flexible honeycomb. In addition, the various models determine the buckling load through the assumption that the edges of the sandwich panel are in-plane unrestrained (movable support) at the buckling stage and restrained (immovable) at the prebuckling stage, which contradicts the real restrained boundary conditions. This contradiction is based on the assumption used by many researchers, but which is unsubstantiated, that the in-plane compressive stress resultants at the buckling stage do not change. In the case of a sandwich panel with a soft core that may expand or contract, this assumption is generally incorrect.

The present analysis incorporates the effects of the flexible core, as well as its thermal strain in the vertical direction, into the mathematical models and follows the high-order sandwich-panel theory approach. The variational principle of minimum of the total potential energy is used to derive the field equations and the appropriate boundary conditions. The prebuckling and the buckling governing equations are defined through a perturbation technique (see Simitses [27]) that yields a set of linearized equations, and their closed-form solution for a specific simply supported panel is presented.

The formulation is based on the well-known assumptions for sandwich structures with soft/compliant cores:

1) The face sheets have in-plane and bending rigidities; the face sheets and the core material are assumed be linear elastic.

2) The face sheets undergo large displacements and moderate rotations (geometrically nonlinear).

3) The core is considered as a 2-D linear elastic medium with kinematic relations corresponding to small deformations (geometrically linear), for which the core height may change during deformation, and its section planes do not remain plane after deformation.

4) The core possesses only shear and transverse normal stiffness, whereas the in-plane (longitudinal) normal stiffness is assumed to be nil.

5) Thermal fields are applied to the face sheets and the core without a change in their mechanical properties and the thermal conductivity of the face sheets, and the core is unaffected by the temperature field.

6) The mechanical loads are applied to the face sheets only.

This paper first presents a nonlinear analysis of sandwich panels subjected to thermally induced deformation. The field equations and the appropriate boundary conditions are derived through a variational approach. A perturbation technique is used to linearize the nonlinear field equations and to define the equations for the prebuckling and the buckling states. A simplified closed-form solution is presented for a specific simply supported sandwich panel, while neglecting the expansion/contraction thermal strains of the core. These simplified solutions are compared with the full nonlinear solutions, and the effects of the core strains on the buckling and the postbuckling responses are presented through numerical examples. Finally, conclusions are presented.

Nonlinear Thermal Governing Equations

The set of the nonlinear field equations used for the analysis herein is based on the kinematic relations corresponding to large displacement with moderate rotations. They were derived through the minimization of the total potential energy following the procedure presented in Frostig and Baruch [23] (see also Frostig and Thomsen [28]). The closed-form description of the stress and displacement fields of the core appears in Frostig [22] and is briefly presented here for completeness.

The set of the nonlinear thermal governing equations was derived using the procedure outlined in Frostig and Baruch [23] and the following isotropic constitutive relation:

For the upper- and the lower-face sheets:

$$\frac{\sigma_{xxj}(x,z_j)}{E_j}=\left(\frac{\mathrm{d}}{\mathrm{d}x}u_{oj}(x)\right)-\left(\frac{\mathrm{d}^2}{\mathrm{d}x^2}w_j(x)\right)z_j+\frac{1}{2}\left(\frac{\mathrm{d}}{\mathrm{d}x}w_j(x)\right)^2-\alpha_j\left(\frac{1}{2}T_{j_t}(x)+\frac{1}{2}T_{j_b}(x)+\frac{(T_{j_b}(x)-T_{j_t}(x))z_j}{d_j}\right)\qquad(j=t,b)\tag{1}$$

For the core:

$$\frac{\sigma_{zz}(x,z_c)}{E_{zc}}=\left(\frac{\partial}{\partial z_c}w_c(x,z_c)\right)-\alpha_c\left(T_{c_t}(x)\left(1-\frac{z_c}{c}\right)+\frac{T_{c_b}(x)z_c}{c}\right)\tag{2}$$

$$\frac{\tau_c(x,z_c)}{G_{xzc}}=\left(\frac{\partial}{\partial z_c}u_c(x,z_c)\right)+\left(\frac{\partial}{\partial x}w_c(x,z_c)\right)\tag{3}$$

where the following definitions refer to the two face sheets ($j=t,b$): $\sigma_{xxj}(x,z_j)$ are the longitudinal normal stresses; w_j and u_{oj} are the vertical and midplane in-plane displacements; E_j is the modulus of elasticity; d_j is the thickness of the face sheet; α_j is the coefficient of thermal expansion (CTE) of the face sheets; $T_{j_k}(x)$ and $(k=t,b)$ are the temperatures at the upper and lower fibers of the faces, respectively; z_j is the vertical coordinate of the faces measured downward from centroid of each face sheet separately; and x is the longitudinal coordinate of the sandwich panel. The terms related to the core are $\tau_c(x,z_c)$; $\sigma_{zz}(x,z_c)$ are the shear and the vertical normal stresses; E_{zc} and G_{xzc} are the vertical modulus of elasticity and the shear modulus; $w_c(x,z_c)$ and $u_c(x,z_c)$ are the vertical and in-plane displacements, respectively; α_c is the coefficient of thermal expansion; $T_{c_k}(x)$ and $(k=t,b)$ are the temperatures at the upper and lower fibers of the core, respectively; c is the core height; and z_c is the vertical coordinate measured from the upper-face–core interface (see Fig. 2 for sign conventions and temperatures distribution). Notice that the temperature at the adjacent face of the core and the face sheets are not identical, and thus $T_{c_t}\neq T_{t_b}$ and $T_{c_b}\neq T_{b_t}$ (see the temperature distribution in Fig. 2). Hence, the nonlinear thermal governing equations for the sandwich panel that consist of equilibrium equations, constitutive relations, and a compatibility equation of the longitudinal displacements at the lower-face–core interface read

$$-n_{xt}-\left(\frac{\mathrm{d}}{\mathrm{d}x}N_{xxt}(x)\right)-\tau(x)b_w=0\tag{4}$$

$$N_{xxt}(x)-EA_t(x)\left(\left(\frac{\mathrm{d}}{\mathrm{d}x}u_{ot}(x)\right)+\frac{1}{2}\left(\frac{\mathrm{d}}{\mathrm{d}x}w_t(x)\right)^2\right)+EA_t(x)\alpha_t\left(\frac{1}{2}T_{t_t}(x)+\frac{1}{2}T_{t_b}(x)\right)=0\tag{5}$$

$$\frac{b_wE_{zc}w_t(x)}{c}-\left(\frac{\mathrm{d}}{\mathrm{d}x}N_{xxt}(x)\right)\left(\frac{\mathrm{d}}{\mathrm{d}x}w_t(x)\right)-\frac{b_wE_{zc}w_b(x)}{c}-b_w\left(-\frac{1}{2}E_{zc}T_{c_b}(x)-\frac{1}{2}E_{zc}T_{c_t}(x)\right)\alpha_c+\left(-\frac{1}{2}b_wd_t-\frac{1}{2}b_wc\right)\left(\frac{\mathrm{d}}{\mathrm{d}x}\tau(x)\right)+\left(\frac{\mathrm{d}}{\mathrm{d}x}m_t(x)\right)-N_{xxt}(x)\left(\frac{\mathrm{d}^2}{\mathrm{d}x^2}w_t(x)\right)-\left(\frac{\mathrm{d}^2}{\mathrm{d}x^2}M_{xxt}(x)\right)-q_t=0\tag{6}$$

$$V_{xzt}(x)-\frac{1}{2}b_wd_t\tau(x)-\left(\frac{\mathrm{d}}{\mathrm{d}x}M_{xxt}(x)\right)-N_{xxt}(x)\left(\frac{\mathrm{d}}{\mathrm{d}x}w_t(x)\right)+m_t(x)=0\tag{7}$$

$$\frac{\mathrm{d}^2}{\mathrm{d}x^2}w_t(x)=-\frac{M_{xxt}(x)}{EI_t(x)}-\frac{\alpha_t(T_{t_b}(x)-T_{t_t}(x))}{d_t}\tag{8}$$

$$-\left(\frac{\mathrm{d}}{\mathrm{d}x}N_{xxb}(x)\right)-n_{xb}+\tau(x)b_w=0\tag{9}$$

$$N_{xxb}(x)-EA_b(x)\left(\left(\frac{\mathrm{d}}{\mathrm{d}x}u_{ob}(x)\right)+\frac{1}{2}\left(\frac{\mathrm{d}}{\mathrm{d}x}w_b(x)\right)^2\right)+EA_b(x)\alpha_b\left(\frac{1}{2}T_{b_t}(x)+\frac{1}{2}T_{b_b}\right)=0\tag{10}$$

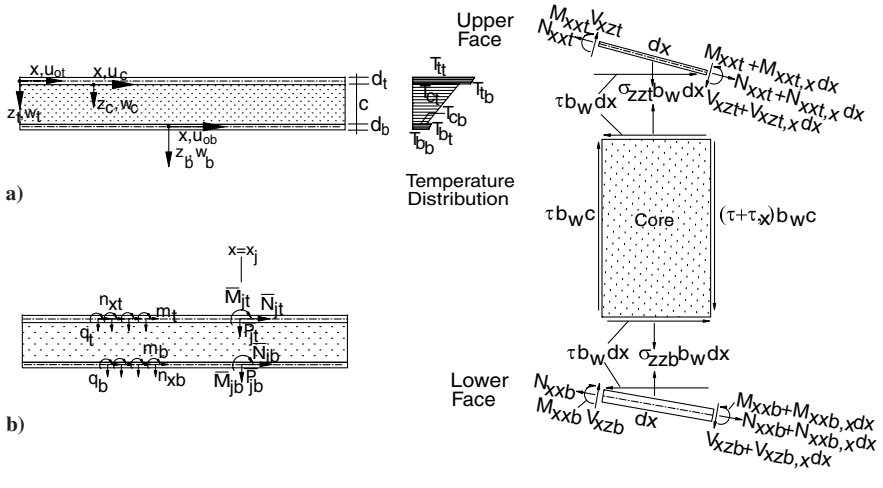

Fig. 2 Geometry, loads, temperature distributions and internal stress resultants: a) geometry, b) external loads, and c) internal stress resultants and interfacial normal stresses.

$$V_{xzb}(x) - \frac{1}{2} b_w d_b \tau(x) - \left(\frac{\mathrm{d}}{\mathrm{d}x} M_{xxb}(x)\right) - N_{xxb}(x)\left(\frac{\mathrm{d}}{\mathrm{d}x} w_b(x)\right) + m_b(x) = 0 \tag{11}$$

$$-\frac{b_w E_{zc} w_t(x)}{c} + \frac{b_w E_{zc} w_b(x)}{c} - \left(\frac{\mathrm{d}}{\mathrm{d}x} N_{xxb}(x)\right)\left(\frac{\mathrm{d}}{\mathrm{d}x} w_b(x)\right) + b_w\left(-\frac{1}{2} E_{zc} T_{c_b}(x) - \frac{1}{2} E_{zc} T_{c_t}(x)\right)\alpha_c + \left(-\frac{1}{2} b_w d_b - \frac{1}{2} b_w c\right)\left(\frac{\mathrm{d}}{\mathrm{d}x}\tau(x)\right) + \left(\frac{\mathrm{d}}{\mathrm{d}x} m_b(x)\right) - q_b - N_{xxb}(x)\left(\frac{\mathrm{d}^2}{\mathrm{d}x^2} w_b(x)\right) - \left(\frac{\mathrm{d}^2}{\mathrm{d}x^2} M_{xxb}(x)\right) = 0 \tag{12}$$

$$\frac{\mathrm{d}^2}{\mathrm{d}x^2} w_b(x) = -\frac{M_{xxb}(x)}{EI_b(x)} - \frac{\alpha_b (T_{b_b}(x) - T_{b_t}(x))}{d_b} \tag{13}$$

$$\left(-\frac{c}{2} - \frac{1}{2} d_t\right)\left(\frac{\mathrm{d}}{\mathrm{d}x} w_t(x)\right) + \left(-\frac{1}{2} d_b - \frac{c}{2}\right)\left(\frac{\mathrm{d}}{\mathrm{d}x} w_b(x)\right) + \left(\frac{1}{12} c^2\left(\frac{\mathrm{d}}{\mathrm{d}x} T_{c_t}(x)\right) + \frac{1}{12} c^2\left(\frac{\mathrm{d}}{\mathrm{d}x} T_{c_c}(x)\right)\right)\alpha_c + \frac{c\tau(x)}{G_{xzc}} - \frac{1}{12}\frac{c^3((\mathrm{d}^2/\mathrm{d}x^2)\tau(x))}{E_{zc}} + u_{ot}(x) - u_{ob}(x) = 0 \tag{14}$$

where the following terms refer to the upper- and lower-face sheets, respectively ($j = t, b$): N_{xxj} and M_{xxj} are the in-plane and bending-moment stress resultants of each face sheet; V_{xzj} are the shear stress resultants in the upper- and lower-face sheets; n_{xj}, q_j, and m_j are the external distributed loads in the longitudinal and vertical directions and the bending moment applied to the upper- and lower-face sheets, respectively; d_j ($j = t, b$) are the thickness of the various face sheets; EA_j and EI_j are the in-plane and flexural rigidity of the various independent face sheets; N_{jk}, P_{jk}, and M_{jk} ($k = t, b$) are the external concentrated loads (in longitudinal and vertical directions) and bending moments applied at $x = xj$ at the various face sheets, respectively; $\tau(x)$ is the shear stress in the core; b_w is the width of the panel; and $\mathrm{d}x$ is the length of a differential segment. For sign conventions of coordinates, stresses, displacements, temperatures distribution, and stress resultants, see Fig. 2. The notation $(\,)_{,x} = (\mathrm{d}/\mathrm{d}x)(\,)$ in Fig. 2 refers to a derivative with respect to x.

The stress and displacement fields of the core were determined through the solutions of the differential equilibrium equations, which are derived by the variational procedure, along with the constitutive relations [see Eqs. (2) and (3)] (for details, see Frostig [22]); they read

$$\tau_c(x, z_c) = \tau(x) \tag{15}$$

$$\sigma_{zz}(x, z_c) = \left(-\frac{w_t(x)}{c} + \frac{w_b(x)}{c} - \frac{1}{2}\alpha_c T_{c_t}(x) - \frac{1}{2}\alpha_c T_{c_b}(x)\right) E_{zc} + \left(-z_c + \frac{c}{2}\right)\left(\frac{\mathrm{d}}{\mathrm{d}x}\tau(x)\right) \tag{16}$$

$$w_c(x, z_c) = \left(\frac{1}{2}\frac{z_c^2}{c}\alpha_c - \frac{1}{2} z_c \alpha_c\right) T_{c_b}(x) + \left(\frac{1}{2} z_c \alpha_c - \frac{1}{2}\frac{z_c^2}{c}\alpha_c\right) T_{c_t}(x) + \left(1 - \frac{z_c}{c}\right) w_t(x) + \frac{z_c w_b(x)}{c} + \frac{(\frac{1}{2} c z_c - \frac{1}{2} z_c^2)((\mathrm{d}/\mathrm{d}x)\tau(x))}{E_{zc}} \tag{17}$$

$$u_c(x, z_c) = \left(-z_c + \frac{1}{2}\frac{z_c^2}{c} - \frac{1}{2} d_t\right)\left(\frac{\mathrm{d}}{\mathrm{d}x} w_t(x)\right) - \frac{1}{2}\frac{z_c^2((\mathrm{d}/\mathrm{d}x) w_b(x))}{c} + \frac{z_c \tau(x)}{G_{xzc}} + \left(\left(\frac{1}{6}\frac{z_c^3}{c} - \frac{1}{4} z_c^2\right)\left(\frac{\mathrm{d}}{\mathrm{d}x} T_{c_t}(x)\right) + \left(-\frac{1}{6}\frac{z_c^3}{c} + \frac{1}{4} z_c^2\right)\left(\frac{\mathrm{d}}{\mathrm{d}x} T_{c_b}(x)\right)\right)\alpha_c + u_{ot}(x) + \frac{(-\frac{1}{4} c z_c^2 + \frac{1}{6} z_c^3)((\mathrm{d}^2/\mathrm{d}x^2)\tau(x))}{E_{zc}} \tag{18}$$

The vertical normal stresses at the upper- and the lower-face–core interfaces read

$$\sigma_{zzt}(x) = \left(-\frac{w_t(x)}{c} + \frac{w_b(x)}{c} - \frac{1}{2}\alpha_c T_{c_t}(x) - \frac{1}{2}\alpha_c T_{c_b}(x)\right) E_{zc} + \frac{1}{2}\left(\frac{\mathrm{d}}{\mathrm{d}x}\tau(x)\right) c \tag{19}$$

$$\sigma_{zzb}(x) = \left(-\frac{w_t(x)}{c} + \frac{w_b(x)}{c} - \frac{1}{2}\alpha_c T_{c_t}(x) - \frac{1}{2}\alpha_c T_{c_b}(x)\right) E_{zc} - \frac{1}{2}\left(\frac{\mathrm{d}}{\mathrm{d}x}\tau(x)\right) c \tag{20}$$

The nonlinear governing equations can be solved numerically after replacing the first ten equations, Eqs. (4–13), with 12 equivalent first-order equations of the following unknowns for the two face sheets: $u_{oj}(x)$, $w_j(x)$, $(\mathrm{d}/\mathrm{d}x) w_j(x)$, $N_{xxj}(x)$, $V_{xzj}(x)$, and $M_{xxj}(x)$ ($j = t, b$) (see Frostig and Thomsen [28] for details). The last governing Eq. (13), which describes the compatibility condition in the longitudinal direction at the lower-face–core interface, is replaced by two first-order equations as follows:

$$\frac{\mathrm{d}}{\mathrm{d}x}\tau(x) = D\tau(x) E_{zc} - \frac{E_{zc}\alpha_c T_{c_t}(x)}{c} + \frac{E_{zc}\alpha_c T_{c_b}(x)}{c} \tag{21}$$

$$\frac{\mathrm{d}}{\mathrm{d}x} D\tau(x) = \left(-\frac{6}{c^2} - \frac{6\,\mathrm{d}t}{c^3}\right)\left(\frac{\mathrm{d}}{\mathrm{d}x} w_t(x)\right) + \left(-\frac{6}{c^2} - \frac{6\,\mathrm{d}b}{c^3}\right)\left(\frac{\mathrm{d}}{\mathrm{d}x} w_b(x)\right) + \frac{12\tau(x)}{c^2 Gc} - \frac{12 u_{ob}(x)}{c^3} + \frac{12 u_{ot}(x)}{c^3} \tag{22}$$

where $D\tau(x)$ is a dummy function that replaces the derivative of the shear stresses [see Eq. (21)] and also enhances the numerical efficiency of the solution.

The boundary and the continuity conditions are based on the 14 unknown functions. The boundary conditions consist of six conditions for each face sheet that follow those of ordinary unidirectional panels or beams and two conditions of the core that require either a free edge with null shear stresses or a constrain on the vertical displacement at the edge of the core through its depth. For details, see Frostig and Thomsen [28] and Frostig [22] for the core.

The postbuckling response is described through the numerical solution of the nonlinear first-order set of differential equations that is solved using the multiple-point shooting method, along with the procedure that implements the natural parametric and pseudo-arc-length continuation methods and is capable of retrieving of secondary bifurcation occurrence (see Stoer and Bulirsch [29] and Keller [30]). The governing equations of the prebuckling and buckling stages are derived next.

Prebuckling and Buckling Stages: Linearized Equations

The nonlinear governing equations are linearized using a perturbation technique (see Simitses [27]) to define the governing equations for the prebuckling and the buckling stages. To achieve a compact yet simple linearized set of equations, the mechanical properties are assumed to be uniform through the length of the sandwich panel, and the nonlinear governing equations [see Eqs. (4–14)] were consolidated into seven equations: Eqs. (4–6) for the upper-face sheet, Eqs. (9–11) for the lower-face sheet, and the compatibility equation (14). The bending stress resultants of the face sheets, $M_{xxj}(j = t, b)$, that appear in the aforementioned equations are replaced by their constitutive relations (8) and (13) for the upper- and lower-face sheets, respectively. Thus, the new set of the governing equations consist of seven unknowns that using the perturbation approach read

$$\begin{aligned} u_{ot}(x) &= u_{ot}(x)^{[o]} + \xi u_{ot}(x)^{[1]}, \qquad u_{ob}(x) = u_{ob}(x)^{[0]} + \xi u_{ob}(x)^{[1]} \\ w_t(x) &= w_t(x)^{[o]} + \xi w_t(x)^{[1]}, \qquad w_b(x) = w_b(x)^{[0]} + \xi w_b(x)^{[1]} \\ N_{xxt}(x) &= N_{xxt}(x)^{[o]} + \xi N_{xxt}(x)^{[1]} \\ N_{xxb}(x) &= N_{xxb}(x)^{[o]} + \xi N_{xxb}(x)^{[1]}, \qquad \tau(x) = \tau(x)^{[o]} + \xi \tau(x)^{[1]} \end{aligned} \tag{23}$$

where $\xi \ll 1$ is the perturbation parameter and the superscripts $[o]$ and [1] refer to the prebuckling and buckling stages, respectively.

The equations for the different stages are derived through substitution of Eqs. (23) into the consolidated set of the governing equations and by collecting the coefficients that correspond to the zeroth power (prebuckling stage) and the first power (buckling stage). Hence, they read as follows:

Prebuckling stage:

$$-n_{xt} - \left(\frac{\mathrm{d}}{\mathrm{d}x} N_{xxt}(x)^{[o]}\right) - b_w \tau(x)^{[o]} = 0 \tag{24}$$

$$\left(-\left(\frac{\mathrm{d}}{\mathrm{d}x} u_{ot}(x)^{[o]}\right) + \alpha_t \left(\frac{1}{2} T_{t_t} + \frac{1}{2} T_{t_b}\right) - \frac{1}{2}\left(\frac{\mathrm{d}}{\mathrm{d}x} w_t(x)^{[o]}\right)^2\right) EA_t + N_{xxt}(x)^{[o]} = 0 \tag{25}$$

$$\begin{aligned} &\left(\left(\frac{(\mathrm{d}^2/\mathrm{d}x^2) T_{t_b}(x)}{d_t} - \frac{(\mathrm{d}^2/\mathrm{d}x^2) T_{t_t}(x)}{d_t}\right)\alpha_t + \left(\frac{\mathrm{d}^4}{\mathrm{d}x^4} w_t(x)^{[o]}\right)\right) EI_t \\ &- \left(\frac{\mathrm{d}}{\mathrm{d}x} N_{xxt}(x)^{[o]}\right)\left(\frac{\mathrm{d}}{\mathrm{d}x} w_t(x)^{[o]}\right) \\ &+ \left(-\frac{c}{2} - \frac{1}{2} d_t\right) b_w \left(\frac{\mathrm{d}}{\mathrm{d}x} \tau(x)^{[o]}\right) + \left(\left(\frac{1}{2} T_{c_b}(x) + \frac{1}{2} T_{c_t}\right)\alpha_c \right. \\ &\left. + \frac{w_t(x)^{[o]}}{c} - \frac{w_b(x)^{[o]}}{c}\right) E_{zc} b_w + \left(\frac{\mathrm{d}}{\mathrm{d}x} m_t(x)\right) \\ &- q_t - N_{xxt}(x)^{[o]}\left(\frac{\mathrm{d}^2}{\mathrm{d}x^2} w_t(x)^{[o]}\right) = 0 \end{aligned} \tag{26}$$

$$-\left(\frac{\mathrm{d}}{\mathrm{d}x} N_{xxb}(x)^{[o]}\right) - n_{xb} + b_w \tau(x)^{[o]} = 0 \tag{27}$$

$$\left(-\left(\frac{\mathrm{d}}{\mathrm{d}x} u_{ob}(x)^{[o]}\right) + \alpha_b \left(\frac{1}{2} T_{b_t}(x) + \frac{1}{2} T_{b_b}\right) - \frac{1}{2}\left(\frac{\mathrm{d}}{\mathrm{d}x} w_b(x)^{[o]}\right)^2\right) EA_b + N_{xxb}(x)^{[o]} = 0 \tag{28}$$

$$\begin{aligned} &\left(\left(\frac{(\mathrm{d}^2/\mathrm{d}x^2) T_{b_b}(x)}{d_b} - \frac{(\mathrm{d}^2/\mathrm{d}x^2) T_{b_t}(x)}{d_b}\right)\alpha_b + \left(\frac{\mathrm{d}^4}{\mathrm{d}x^4} w_b(x)^{[o]}\right)\right) EI_b \\ &+ \left(-\frac{1}{2} d_b - \frac{c}{2}\right) b_w \left(\frac{\mathrm{d}}{\mathrm{d}x} \tau(x)^{[o]}\right) + \left(\left(-\frac{1}{2} T_{c_b}(x) - \frac{1}{2} T_{c_t}\right)\alpha_c \right. \\ &\left. + \frac{w_b(x)^{[o]}}{c} - \frac{w_t(x)^{[o]}}{c}\right) E_{zc} b_w - \left(\frac{\mathrm{d}}{\mathrm{d}x} N_{xxb}(x)^{[o]}\right)\left(\frac{\mathrm{d}}{\mathrm{d}x} w_b(x)^{[o]}\right) \\ &+ \left(\frac{\mathrm{d}}{\mathrm{d}x} m_b(x)\right) - N_{xxb}(x)^{[o]}\left(\frac{\mathrm{d}^2}{\mathrm{d}x^2} w_b(x)^{[o]}\right) - q_b = 0 \end{aligned} \tag{29}$$

$$\begin{aligned} &\left(-\frac{c}{2} - \frac{1}{2} d_t\right)\left(\frac{\mathrm{d}}{\mathrm{d}x} w_t(x)^{[o]}\right) + \left(-\frac{1}{2} d_b - \frac{c}{2}\right)\left(\frac{\mathrm{d}}{\mathrm{d}x} w_b(x)^{[o]}\right) \\ &+ \left(-\frac{1}{12} c^2 \left(\frac{\mathrm{d}}{\mathrm{d}x} T_{c_t}(x)\right) + \frac{1}{12} c^2 \left(\frac{\mathrm{d}}{\mathrm{d}x} T_{c_b}(x)\right)\right)\alpha_c + \frac{c\tau(x)^{[o]}}{G_{xzc}} \\ &- u_{ob}(x)^{[o]} + u_{ot}(x)^{[o]} - \frac{1}{12} \frac{c^3 ((\mathrm{d}^2/\mathrm{d}x^2)\tau(x)^{[o]})}{E_{zc}} = 0 \end{aligned} \tag{30}$$

Buckling stage:

$$-\left(\frac{\mathrm{d}}{\mathrm{d}x} N_{xxt}(x)^{[1]}\right) - b_w \tau(x)^{[1]} = 0 \tag{31}$$

$$N_{xxt}(x)^{[1]} - EA_t(x)\left(\frac{\mathrm{d}}{\mathrm{d}x} w_t(x)^{[o]}\right)\left(\frac{\mathrm{d}}{\mathrm{d}x} w_t(x)^{[1]}\right) - EA_t(x)\left(\frac{\mathrm{d}}{\mathrm{d}x} u_{ot}(x)^{[1]}\right) = 0 \tag{32}$$

$$\begin{aligned} &\frac{b_w E_{zc} w_t(x)^{[1]}}{c} - \frac{b_w E_{zc} w_b(x)^{[1]}}{c} + \left(-\frac{1}{2} b_w d_t - \frac{1}{2} b_w c\right)\left(\frac{\mathrm{d}}{\mathrm{d}x} \tau(x)^{[1]}\right) \\ &- \left(\frac{\mathrm{d}}{\mathrm{d}x} N_{xxt}(x)^{[1]}\right)\left(\frac{\mathrm{d}}{\mathrm{d}x} w_t(x)^{[o]}\right) + EI_t(x)\left(\frac{\mathrm{d}^4}{\mathrm{d}x^4} w_t(x)^{[1]}\right) \\ &- N_{ot}\left(\frac{\mathrm{d}^2}{\mathrm{d}x^2} w_t(x)^{[1]}\right) - N_{xxt}(x)^{[1]}\left(\frac{\mathrm{d}^2}{\mathrm{d}x^2} w_t(x)^{[o]}\right) = 0 \end{aligned} \tag{33}$$

$$-\left(\frac{\mathrm{d}}{\mathrm{d}x} N_{xxb}(x)^{[1]}\right) + b_w \tau(x)^{[1]} = 0 \tag{34}$$

$$N_{xxb}(x)^{[1]} - EA_b(x)\left(\frac{\mathrm{d}}{\mathrm{d}x} w_b(x)^{[o]}\right)\left(\frac{\mathrm{d}}{\mathrm{d}x} w_b(x)^{[1]}\right) - EA_b(x)\left(\frac{\mathrm{d}}{\mathrm{d}x} u_{ob}(x)^{[1]}\right) = 0 \tag{35}$$

$$\begin{aligned} &-\frac{b_w E_{zc} w_t(x)^{[1]}}{c} + \frac{b_w E_{zc} w_b(x)^{[1]}}{c} + \left(-\frac{1}{2} b_w d_b - \frac{1}{2} b_w c\right) \\ &\times \left(\frac{\mathrm{d}}{\mathrm{d}x} \tau(x)^{[1]}\right) - \left(\frac{\mathrm{d}}{\mathrm{d}x} N_{xxb}(x)^{[1]}\right)\left(\frac{\mathrm{d}}{\mathrm{d}x} w_b(x)^{[o]}\right) \\ &+ EI_b(x)\left(\frac{\mathrm{d}^4}{\mathrm{d}x^4} w_b(x)^{[1]}\right) - N_{xxb}(x)^{[1]}\left(\frac{\mathrm{d}^2}{\mathrm{d}x^2} w_b(x)^{[o]}\right) \\ &- N_{ob}\left(\frac{\mathrm{d}^2}{\mathrm{d}x^2} w_b(x)^{[1]}\right) = 0 \end{aligned} \tag{36}$$

$$\begin{aligned} &\left(-\frac{c}{2} - \frac{1}{2} d_t\right)\left(\frac{\mathrm{d}}{\mathrm{d}x} w_t(x)^{[1]}\right) + \left(-\frac{1}{2} d_b - \frac{c}{2}\right)\left(\frac{\mathrm{d}}{\mathrm{d}x} w_b(x)^{[1]}\right) \\ &+ u_{ot}(x)^{[1]} - u_{ob}(x)^{[1]} + \frac{c\tau(x)^{[1]}}{G_{xzc}} - \frac{1}{12} \frac{c^3 ((\mathrm{d}^2/\mathrm{d}x^2)\tau(x)^{[1]})}{E_{zc}} = 0 \end{aligned} \tag{37}$$

where $N_{oj}(j = t, b)$ are the in-plane stress resultants in the face sheets at the prebuckling stage when no external loads are applied to the face sheets [see Eqs. (24) and (27)].

The governing equations corresponding to the prebuckling stage are generally nonlinear, and no general analytical closed-form solution exists. The computational efforts associated with their numerical solution are of the same order as the solution of the original nonlinear set of equations. Notice that, in general, the prebuckling stage describes a membrane state, even in the absence of external loads.

Simplified Solution: Vertical Core Expansion/ Contraction Neglected

When no external loads are present and the thermal expansion or contraction of the core in the vertical direction is neglected or yields only rigid-body movements (see Fig. 1a), a simplified solution is possible, and a membrane state at the prebuckling stage exists. In such a case, the prebuckling equations reduces to the following set of equations:

$$\begin{aligned}
&\tau(x)^{[o]} = 0, \qquad w_t(x)^{[o]} = 0, \qquad w_b(x)^{[o]} = 0\\
&\qquad -\left(\frac{\mathrm{d}}{\mathrm{d}x} N_{xxt}(x)^{[o]}\right) = 0\\
&N_{xxt}(x)^{[o]} - EA_t\left(\frac{\mathrm{d}}{\mathrm{d}x} u_{ot}(x)^{[o]}\right) + EA_t\alpha_t\left(\frac{1}{2}T_{t_t} + \frac{1}{2}T_{t_b}\right) = 0\\
&\qquad -\left(\frac{\mathrm{d}}{\mathrm{d}x} N_{xxb}(x)^{[o]}\right) = 0\\
&N_{xxb}(x)^{[o]} - EA_b\left(\frac{\mathrm{d}}{\mathrm{d}x} u_{ob}(x)^{[o]}\right) + EA_b\alpha_b\left(\frac{1}{2}T_{b_t} + \frac{1}{2}T_{b_b}\right) = 0\\
&\qquad -u_{ob}(x)^{[o]} + u_{ot}(x)^{[o]} = 0
\end{aligned} \tag{38}$$

where the last equation is equivalent to the requirement that the midplane strain must be identical in the upper- and lower-face sheets. The analytical closed-form solution of this set of equations, in the case of a uniformly distributed thermal loading along the panel, uniform mechanical properties, and edges that are restrained in the in-plane direction (see Fig. 1), reads

$$\begin{aligned}
&u_{ot}(x)^{[o]} = 0, \qquad N_{xxt}(x)^{[o]} = -EA_t\alpha_t(\tfrac{1}{2}T_{t_t} + \tfrac{1}{2}T_{t_b})\\
&u_{ob}(x)^{[o]} = 0, \qquad N_{xxb}(x)^{[o]} = -EA_b\alpha_t(\tfrac{1}{2}T_{t_t} + \tfrac{1}{2}T_{t_b})
\end{aligned} \tag{39}$$

where $N_{oj} = N_{xxj}(j = t, b)$ [see Eqs. (33) and (36)].

The buckling-stage equations (32), (33), (35), and (36) change upon substitution of Eqs. (38) and (39), respectively, as follows:

$$N_{xxt}(x)^{[1]} - EA_t\left(\frac{\mathrm{d}}{\mathrm{d}x} u_{ot}(x)^{[1]}\right) = 0 \tag{40}$$

$$N_{xxb}(x)^{[1]} - EA_b\left(\frac{\mathrm{d}}{\mathrm{d}x} u_{ob}(x)^{[1]}\right) = 0 \tag{42}$$

$$\begin{aligned}
&-\frac{b_w E_{zc} w_t(x)^{[1]}}{c} + \frac{b_w E_{zc} w_b(x)^{[1]}}{c} + \left(-\frac{1}{2}b_w d_b - \frac{1}{2}b_w c\right)\\
&\times\left(\frac{\mathrm{d}}{\mathrm{d}x}\tau(x)^{[1]}\right) + EI_b\left(\frac{\mathrm{d}^4}{\mathrm{d}x^4} w_b(x)^{[1]}\right) - N_{ob}\left(\frac{\mathrm{d}^2}{\mathrm{d}x^2} w_b(x)^{[1]}\right) = 0
\end{aligned} \tag{43}$$

Hence, the updated linear set of equations for the buckling stage consists of Eqs. (31), (34), and (40–43) and Eq. (37). This set of equations is homogeneous, and it can be solved for various boundary conditions either in a closed form or using well-known classical solutions of linear differential equations with constants coefficients. Notice that these equations were derived assuming that the supports are immovable in the in-plane direction. A simple analytical solution exists when a simply supported panel is considered.

Case Study: Simply Supported Sandwich Panel

In the case of a simply supported sandwich panel (see Fig. 1b), the edges of the upper and the lower edges of the face sheets are pinned (with in-plane restrains), and the vertical displacements at the edges of the core through its height are prevented.

The analytical solution consists of a set of functions that fulfill the appropriate boundary conditions of the vertical displacements and also allow horizontal movements of the supports, and they read

$$\begin{aligned}
&u_{ot}(x)^{[1]} = C_{uo_t}\cos\left(\frac{m\pi x}{L}\right), \qquad w_t(x)^{[1]} = C_{w_t}\sin\left(\frac{m\pi x}{L}\right)\\
&u_{ob}(x)^{[1]} = C_{uo_b}\cos\left(\frac{m\pi x}{L}\right), \qquad w_b(x)^{[1]} = C_{w_b}\sin\left(\frac{m\pi x}{L}\right)\\
&\qquad \tau(x)^{[1]} = C_\tau\cos\left(\frac{m\pi x}{L}\right)
\end{aligned} \tag{44}$$

where m is the number of half-waves in the trigonometric functions. The number of unknowns is consolidated to five through substitution of the constitutive relations of the in-plane stress resultants, Eqs. (40) and (42), into Eqs. (31) and (34). Hence, after substitution of Eq. (44) into the buckling equations, these change into an algebraic set of equations that can be described in matrix form as follows:

$$\mathbf{A}\mathbf{f} = \mathbf{0} \tag{45}$$

where $\mathbf{A}$ is a matrix and $\mathbf{f}$ is the vector of unknowns, as follows:

$$\mathbf{A} = \begin{bmatrix}
\frac{EA_t m^2\pi^2}{L^2}, & 0, & 0, & 0, & -b_w\\
0, & \frac{m^2\pi^2 N_{ot}}{L^2} + \frac{b_w E_{zc}}{c} + \frac{m^4\pi^4 EI_t}{L^4}, & 0, & -\frac{b_w E_{zc}}{c}, & \frac{1}{2}\frac{m\pi b_w d_t}{L} + \frac{1}{2}\frac{m\pi b_w c}{L}\\
0, & 0, & \frac{EA_b m^2\pi^2}{L^2} & 0, & b_w\\
0, & -\frac{b_w E_{zc}}{c}, & 0, & \frac{b_w E_{zc}}{c} + \frac{m^4\pi^4 EI_b}{L^4} + \frac{m^2\pi^2 N_{ob}}{L^2}, & \frac{1}{2}\frac{m\pi b_w d_b}{L} + \frac{1}{2}\frac{m\pi b_w c}{L}\\
1, & -\frac{1}{2}\frac{m\pi d_t}{L} - \frac{m\pi c}{2L}, & -1, & -\frac{1}{2}\frac{m\pi d_b}{L} - \frac{m\pi c}{2L}, & \frac{c}{G_{xzc}} + \frac{1}{2}\frac{c^3 m^2\pi^2}{E_{zc}L^2}
\end{bmatrix} \tag{46}$$

$$\begin{aligned}
&\frac{b_w E_{zc} w_t(x)^{[1]}}{c} - \frac{b_w E_{zc} w_b(x)^{[1]}}{c} + \left(-\frac{1}{2}b_w d_t - \frac{1}{2}b_w c\right)\\
&\times\left(\frac{\mathrm{d}}{\mathrm{d}x}\tau(x)^{[1]}\right) + EI_t\left(\frac{\mathrm{d}^4}{\mathrm{d}x^4} w_t(x)^{[1]}\right) - N_{ot}\left(\frac{\mathrm{d}^2}{\mathrm{d}x^2} w_t(x)^{[1]}\right) = 0
\end{aligned} \tag{41}$$

$$\mathbf{f} = [C_{uo_t}, C_{w_t}, C_{uo_b}, C_{w_b}, C_\tau]^T, \qquad \mathbf{0} = [0, 0, 0, 0, 0]^T \tag{47}$$

Notice that by multiplying the last row of matrix $\mathbf{A}$ by $-b_w$, the matrix becomes symmetric. In the case of two identical face sheets and a uniform thermal field through the depth and length of the panel, the prebuckling in-plane stress resultants are equal, and thus

$N_{ob} = N_{ot}$. The critical loads are determined through the requirement that the determinant of the matrix $\mathbf{A}$ must be equal to zero. The critical temperatures are related to the buckling in-plane stress resultants, through the solution of the prebuckling equations [see Eqs. (39)], assuming immovable supports. The critical temperatures and their eigenvectors equal

$$T_{\mathrm{cr,wr}} = \frac{m^4\pi^4 EI_t c + 2b_w E_{zc} L^4}{L^2 m^2 \pi^2 c E A_t \alpha_t}, \qquad \mathbf{f}_{\mathrm{wr}} = [0, -1, 0, 1, 0] \quad (48)$$

$$\begin{aligned} T_{\mathrm{cr,gl}} &= m^2\pi^2 (EI_t EA_t G_{xzc} m^4 c^3 \pi^4 + 12 EA_t L^2 E_{zc} m^2 c \pi^2 EI_t \\ &\quad + 24 EI_t b_w L^4 E_{zc} G_{xzc} + 6 b_w EA_t L^4 E_{zc} G_{xzc} c^2 \\ &\quad + 12 c b_w EA_t d_t L^4 E_{zc} G_{xzc} \\ &\quad + 6 b_w EA_t d_t^2 L^4 E_{zc} G_{xzc}) / (L^2 (24 b_w L^4 E_{zc} G_{xzc} \\ &\quad + m^4 \pi^4 c^3 EA_t G_{xzc} + 12 m^2 \pi^2 c EA_t L^2 E_{zc}) EA_t \alpha_t) \end{aligned}$$

$$\begin{aligned} f_{\mathrm{gl}} = \Bigg[& -1, \\ & -\frac{1}{12}\frac{24 b_w L^4 E_{zc} G_{xzc} + m^4\pi^4 c^3 EA_t G_{xzc} + 12 m^2\pi^2 c EA_t L^2 E_{zc}}{m\pi E_{zc} L^3 G_{xzc} (d_t + c) b_w}, \\ & 1, \frac{1}{12}\frac{24 b_w L^4 E_{zc} G_{xzc} + m^4\pi^4 c^3 EA_t G_{xzc} + 12 m^2\pi^2 c EA_t L^2 E_{zc}}{m\pi E_{zc} L^3 G_{xzc} (d_t + c) b_w}, \\ & -\frac{EA_t m^2 \pi^2}{b_w L^2} \Bigg] \end{aligned} \quad (49)$$

where $T_{\mathrm{cr,wr}}$ and $T_{\mathrm{cr,gl}}$ are the critical temperatures that cause buckling, and they correspond to the local wrinkling type of buckling, in which the two faces move vertically in opposite direction (see $\mathbf{f}_{\mathrm{wr}}$ in Eq. (48), and to global type of buckling, in which the two faces move vertically in the same direction [see $\mathbf{f}_{\mathrm{gl}}$ in Eq. (49)], respectively. The m value that corresponds to the extremum magnitudes of these temperatures is determined through the requirement that their derivative with respect to m must be zero. The wrinkling results within the assumptions of the simplified model can also be determined through a simple model of isolated face sheets that rest on a Winkler type of elastic foundation with a spring coefficient of $k_w = 2E_{cz}/c$ (see, for example, Zenkert [3]). Notice that the values of the critical temperatures do not depend on the CTEs of the core at all. In general, a correct buckling analysis must consider the global and the wrinkling results to define the critical temperatures.

Notice that the simple analytical closed-form solution presented assumes that a membrane state of stress exists at the prebuckling stage due to the omission of the vertical thermal-induced deformations of the core, and it also violates the in-plane restraint conditions at the supports at the buckling stage. In addition, when the expansion or contraction of the core in the vertical direction is considered and a membrane state accordingly cannot exist at the prebuckling stage, the efforts involved with the solution corresponding to the linearized approach and the full nonlinear analysis are of the same order of difficulty. Hence, the simplified solutions should be used with caution in their own right, and they may serve as an initial trial solution for the nonlinear model in general. The quality of the solution is to be determined through comparisons with the full nonlinear solution.

Thermal Postbuckling: Numerical Study

In the practical design of many sandwich panels, the buckling load may serve as the limit load level. Thus, the panel may buckle under service conditions, whereas the collapse of the panel determines the ultimate carrying capacity of the panel. This design approach is possible only if the behavior beyond buckling (i.e., postbuckling) is stable. In general, a unidirectional sandwich panel with a soft core when subjected to in-plane compressive loads may display different types of postbuckling behavior: a columnlike behavior in which the displacement may reach extremely large values with only very small changes in the compressive loads (unstable behavior), a platelike behavior in which any changes in the displacements depend on an increase of the compressive loads (stable behavior), and a shell-like behavior with a limit point for which any change in the displacement requires a reduction in the compressive loads and yields a snap-through phenomenon (unstable behavior) (see Sokolinsky and Frostig [25]).

Therefore, in the design of platelike structures, the sandwich panel may buckle under service conditions, and its ultimate load-carrying capacity corresponds to the collapse load, whereas in the other cases of unidirectional or shell-type sandwich panels, the ultimate carrying capacity corresponds to the buckling load or limit load level. The exact nature of the thermal postbuckling of a unidirectional sandwich panel is of great importance to its design and when assessing the structural safety.

The thermal postbuckling behavior of a typical sandwich panel is presented through the solution of the full nonlinear governing equations with and without the effects of the expansion or contraction of the core in the vertical direction. The nonlinear results in the vicinity of the linearized critical temperatures are compared with the linearized results, as well as with FE results using ANSYS [31] for the assessment of the inefficiencies of the linearized model. To achieve this goal, the imperfection loads, layout, and magnitude were chosen to yield the linearized buckling modes in the vicinity of their critical temperatures for the case of a null CTE in the core, and they are also used for the cases with the nonzero CTEs of the core. These imperfection loads yield an imperfection pattern that corresponds to the overall, or wrinkling, buckling mode. Notice that these loads have also been used to determine the equilibrium path curves for the various CTEs. The ANSYS run used the kinematics of large displacements and large rotations, along with plane stress constitutive relations, and they are presented along the panel and the equilibrium curve of the overall buckling case for the case with the largest CTE that equals 35e–5.

The numerical study investigates the effects of the vertical thermal strain of the core on the nonlinear response in the vicinity of the critical temperatures, which does not depend on the CTEs of the core [see Eqs. (48)] when subjected to thermal fields for two different types: a uniform thermal field and a thermal gradient through the depth of the core.

The study is performed on a sandwich panel with a soft core (see Fig. 3a) that consists of two face sheets made of aramid (Kevlar) with an equivalent modulus of elasticity of 27,400 MPa; a coefficient of thermal expansion of 0.6e–5; and a core made of rock wool with a modulus of elasticity of $E_{zc} = 0.525$ MPa, a shear modulus of 0.212 MPa, and a coefficient of thermal expansion α_C that attains the values 0, 3.5e–5, and 35e–5 for case study 1. For case study 2, α_C is assumed to be 35e–5.

In the first case, the effects of the vertical thermal strains of the core are studied for the wrinkling and global modes of buckling, and the results are presented in Fig. 3–5 for wrinkling buckling and in Figs. 6–8 for global buckling. The linearized analysis, which neglects the thermal strains of the core in the vertical direction, yields a critical temperature of $T_{\mathrm{cr,wr}} = 96.57°\mathrm{C}$ ($N_{o,\mathrm{wr}} = -476.63$ N), with a mode that consists of 11 half-waves for wrinkling buckling and a critical temperature of $T_{\mathrm{cr,gl}} = 25.59°\mathrm{C}$ ($N_{o,\mathrm{gl}} = -126.29$ N) and with a mode that consists of one half-wave for global buckling.

The geometry, imperfection loads, and thermal distribution for the wrinkling buckling appears in Fig. 3a. The deformed shape at a temperature of 99.5°C, which is at the upper range of temperatures for the wrinkling case (see Fig. 5) within the postbuckling range, consists of 11 half-waves in each face sheet, with a mode that is symmetric relative to the core midsurface. The imperfection loads that consist of two concentrated loads at midspan and that act in opposite directions (see Fig. 3a) are introduced to initiate postbuckling with a wrinkling mode.

The results for the different coefficients of thermal expansion of the core at a temperature of 99.5°C at the upper range of temperatures and above the critical wrinkling temperature along the half-span of the panel appear in Fig. 4. The vertical displacements of the two face sheets are equal in magnitude but in opposite directions (see Fig. 4a).

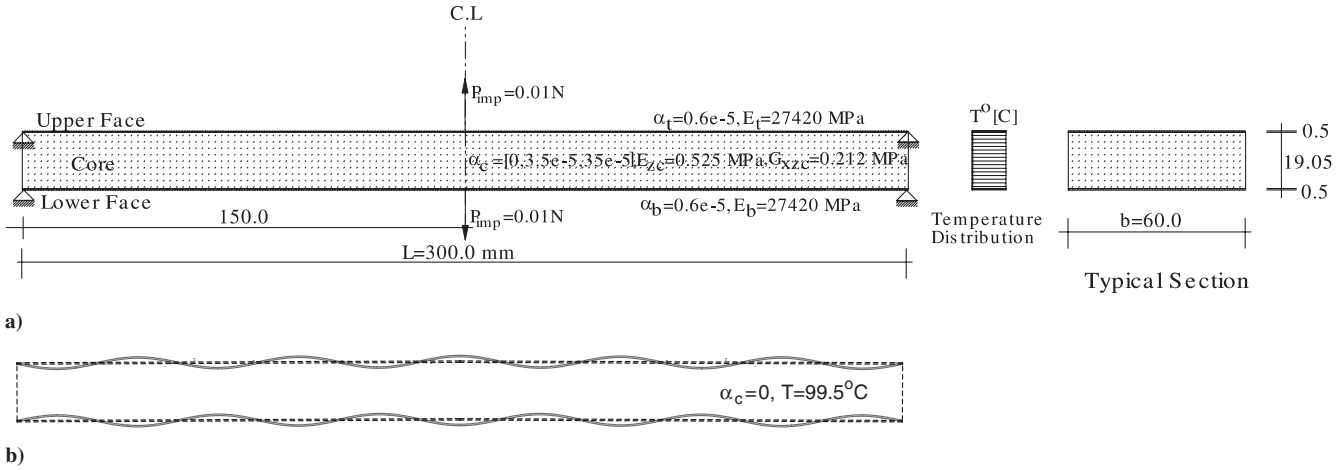

Fig. 3 Geometry and deformed shape of a wrinkled panel with a uniform thermal distribution: a) geometry and mechanical properties and b) deformed shape in the postbuckling range with neglected thermal core strain.

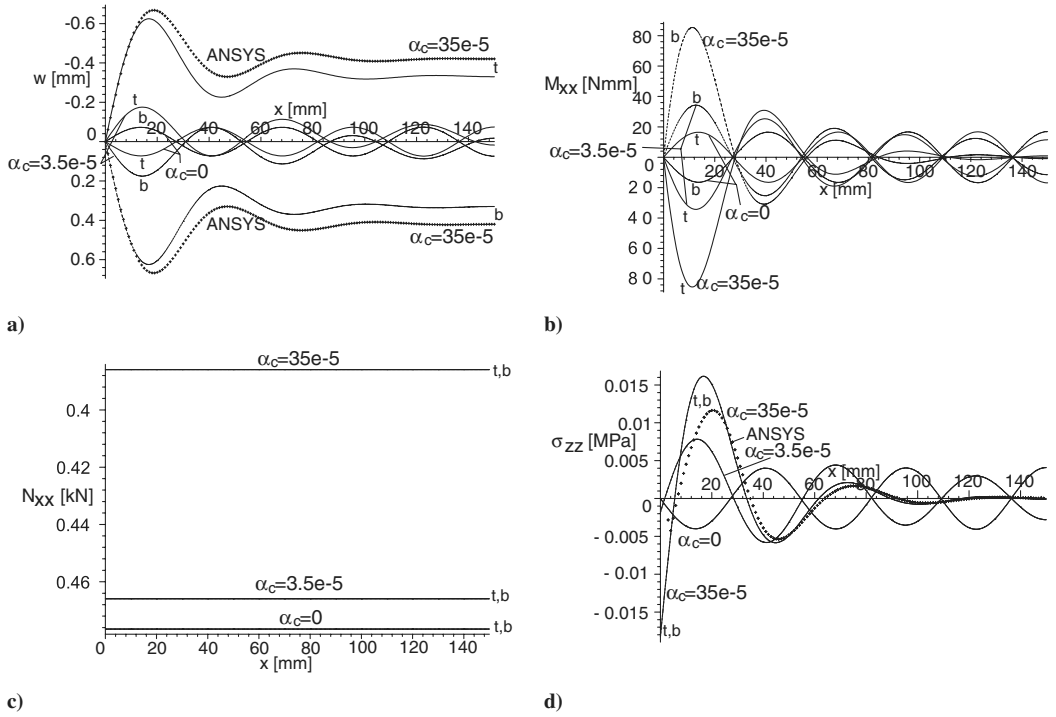

Fig. 4 Results of a wrinkled sandwich panel at $T = 99.5°C$ for various coefficients of expansion of the core: a) vertical displacements, b) bending moments, c) in-plane stress resultants, d) interfacial vertical normal stresses at interfaces; *t* upper-face interface (solid line), *b* lower-face interface (dashed line), and FE (ANSYS) (+).

The value of the extreme displacement obtained for $\alpha_C = 0$ is almost one-tenth of that with a nonzero coefficient. In the first case, with $\alpha_C = 0$, the displacement pattern consists of five-and-a-half half-waves with identical amplitude; in the second case, the half-wave pattern has different values; and in the third case, with the largest value of α_C, the pattern is not periodic at all. The FE results by ANSYS reveal a very similar displacement layout, which coincides near the edge of the panel and is a little bit larger far from the edge. The differences between the results of the two different approaches are due to the large displacement and rotation kinematic relations used by ANSYS, compared with the large displacement and moderate rotations used here. The bending moments for the two face sheets are identical in values but opposite in signs (see Fig. 4b). They are generally periodic for all cases, but with increasing magnitude as α_C increases. The in-plane stress resultants are compressive, identical in the two faces, uniform through the length of the sandwich panel, and reach the critical load of $N_{o,\mathrm{wr}} = -476.63$ N only for $\alpha_C = 0$. In all other cases (i.e., with higher α_C values), the in-plane resultants are smaller. The vertical normal interfacial stresses at the upper- and lower-face–core interfaces are identical, with a periodic pattern, and their magnitude increases as the α_C increases. Also in this case, the ANSYS results compare well with those of the proposed analysis.

The equilibrium curves of temperature vs extreme values for the three different values of α_C appear in Fig. 5, and they were determined using the imperfection loads that appear in Fig. 3a. In the case of $\alpha_C = 0$, a significant change in the pattern of the curve is observed in the vicinity of the critical temperature $T_{\mathrm{cr,wr}}$, determined through the solution of the linearized equations. The curves for vertical displacements of the two face sheets are identical and appear in Fig. 5a. The displacement patterns in the case with nonzero values of α_C are smooth, without any changes in the vicinity of the critical temperature. Notice that in the case of $\alpha_C = 0$, the equilibrium curve presents a typical curve of a plate, with a significant change in the vicinity of the critical temperature and a stable postbuckling curve in which the displacements increase only when the temperature is

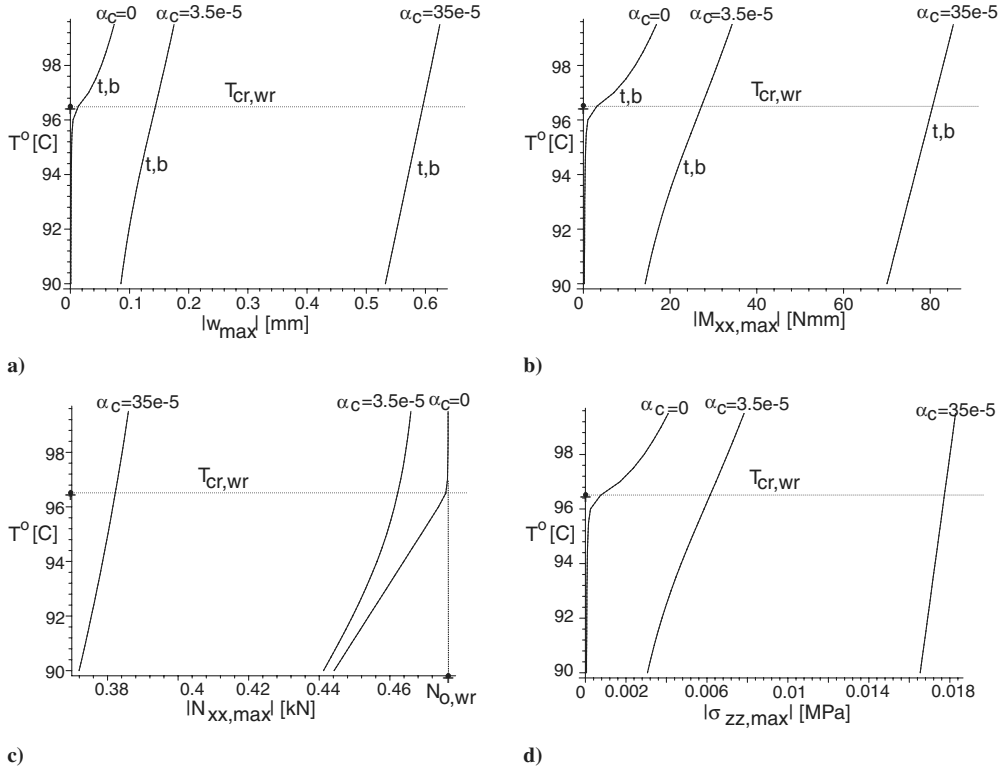

Fig. 5 Nonlinear response curves, temperature vs extreme values of a wrinkled sandwich panel: a) vertical displacements, b) bending moments, c) in-plane compressive stress resultants, and d) interfacial vertical normal stresses at interfaces; *t* upper-face interface (solid line) and *b* lower-face interface (dashed line).

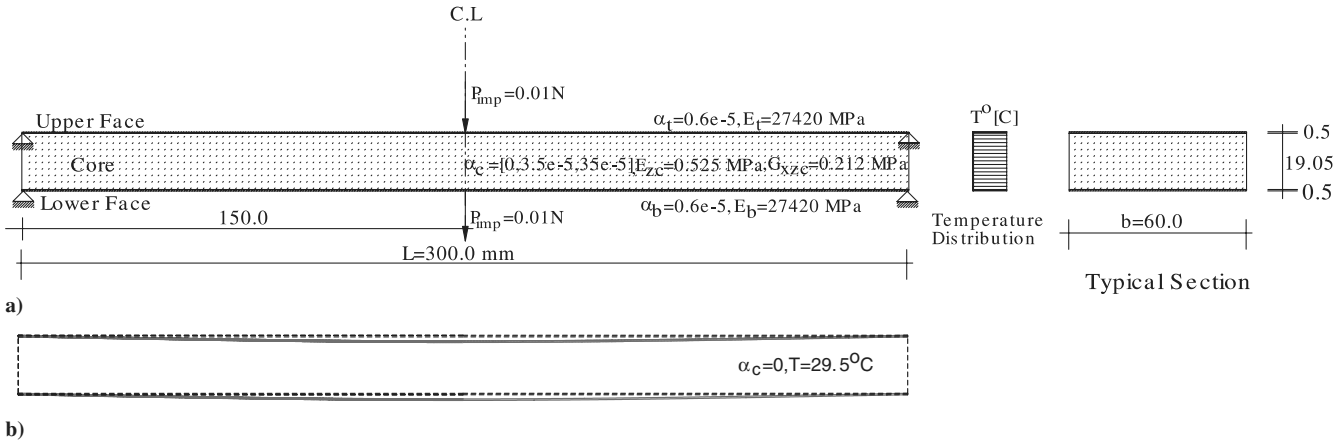

Fig. 6 Geometry and deformed shape of a global buckled sandwich panel with a uniform thermal distribution: a) geometry and mechanical properties and b) deformed shape in the postbuckling range with neglected thermal core strain.

raised. For the other cases (nonzero α_C), the behavior is nonlinear and does not exhibit a buckling phenomenon at all. The maximum bending moments (see Fig. 5b) and the extreme vertical normal interfacial stresses (see Fig. 5d) follow the same trends.

The curves of the in-plane compressive stress resultants appear in Fig. 5c. For the case of $\alpha_C = 0$, the resultants do not change as the temperature is raised. They reach a maximum magnitude that equals the buckling load $N_{o,\mathrm{wr}} = -0.476$ kN corresponding to the linearized model. In the other cases (i.e., for nonzero α_C), the compressive resultants are smaller than the specified critical value. Notice that in the case of $\alpha_C = 0$, the face sheets are subjected to compressive resultants that are a result of the thermal in-plane strains in the face sheets only. In the other cases, with nonzero α_C and with a vertical expansion (see the deformed shape in Fig. 1b), the face sheets elongate, thus yielding tensile stress resultants as a result of the in-plane restraints at the supports. In addition, the face sheets are also subjected to in-plane thermal strains that yield compressive stress resultants, again as a result of the same in-plane restraints. Thus, the in-plane stress resultants in the face sheets are a combination of the compressive and the tensile resultants. Notice that as the temperature is raised, the tensile and the compressive resultants increase. Therefore, when the vertical thermal strains of the core are considered, the panel may exhibit a general nonlinear behavior, rather than buckling in a classical sense. Thus, the approach of the elastic foundation that determines the critical temperature or loads (assuming a buckling phenomenon and using isolated face sheets, while ignoring the vertical thermal strains of the core) is generally inconsistent with the constraints of the problem and is therefore incorrect.

The results of the overall buckling type with a uniform thermal field consists of deformed patterns of the two face sheets that move in the same direction for the different α_C values (see Figs. 6–8). Here, the imperfection concentrated loads are exerted on the upper- and lower-face sheets in the same direction (see Fig. 6a). The deformed

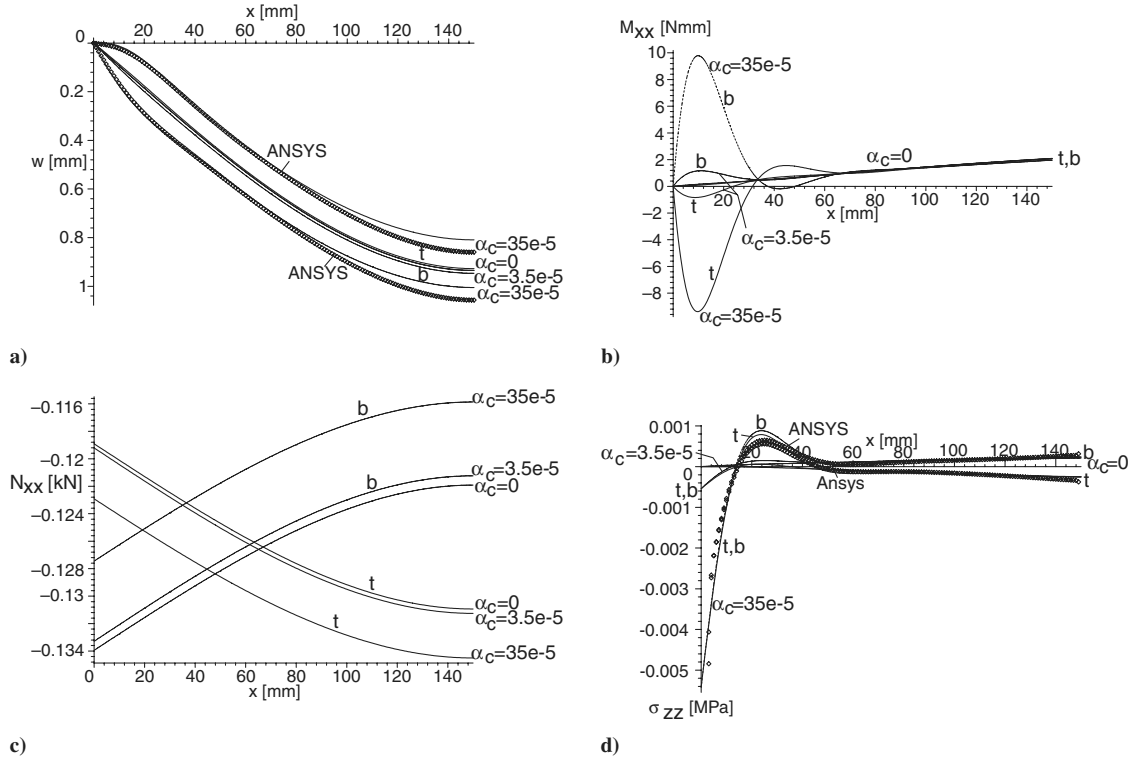

Fig. 7 Results of a global buckled sandwich panel at $T = 29.5°$C for various coefficients of expansion of the core: a) vertical displacements, b) bending moments, c) in-plane stress resultants, and d) interfacial vertical normal stresses at interfaces; *t* upper-face interface (solid line), *b* lower-face interface (dashed line), and FE (ANSYS) (⋄).

shape with $\alpha_C = 0$ that neglects the vertical thermal stresses of the core at a temperature of 29.5°C, which is again at the upper range of temperatures for the overall buckling case (see Fig. 8), appears in Fig. 6b and consists of one half-wave.

The results for the different values of α_C at a temperature of 29.5°C, at the upper range of temperatures along the half-span of the panel, appear in Fig. 7. The vertical displacements of the two face sheets appear in Fig. 7a, and it is observed that they are quite large in

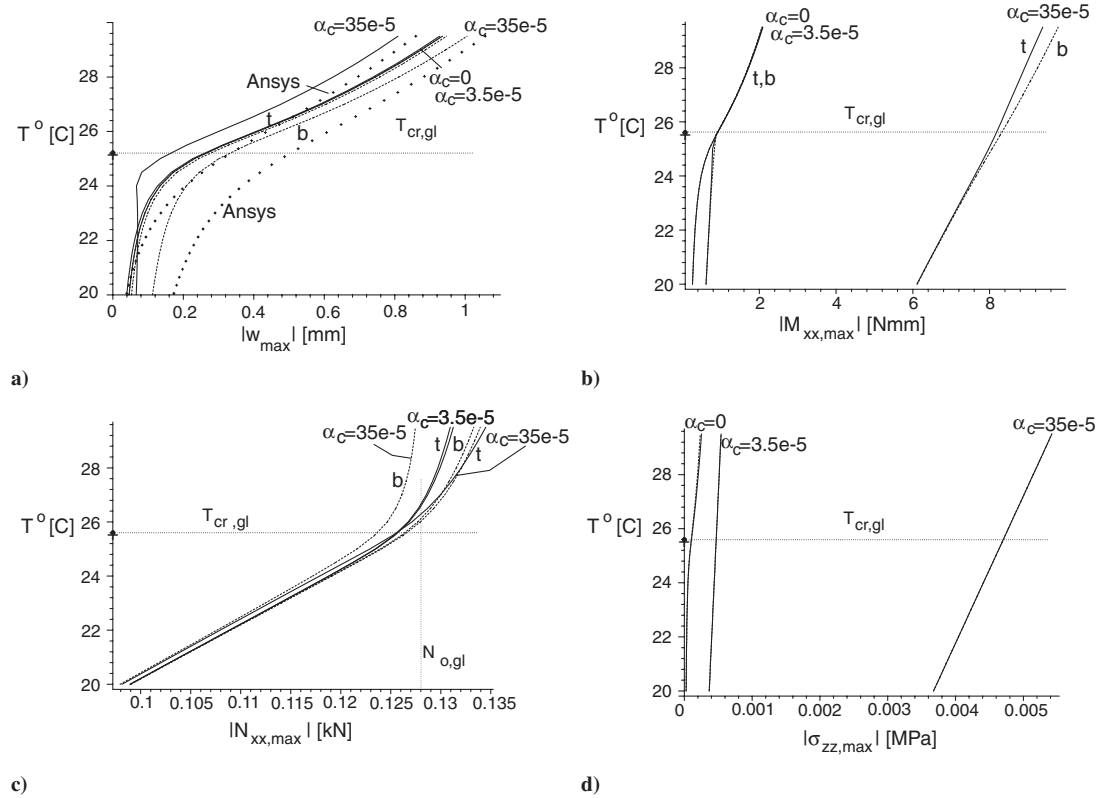

Fig. 8 Nonlinear response curves, temperature vs extreme values of a wrinkled sandwich panel: a) vertical displacements, b) bending moments, c) in-plane compressive stress resultants, and d) interfacial vertical normal stresses at interfaces; *t* upper-face interface (solid line) and *b* lower-face interface (dashed line).

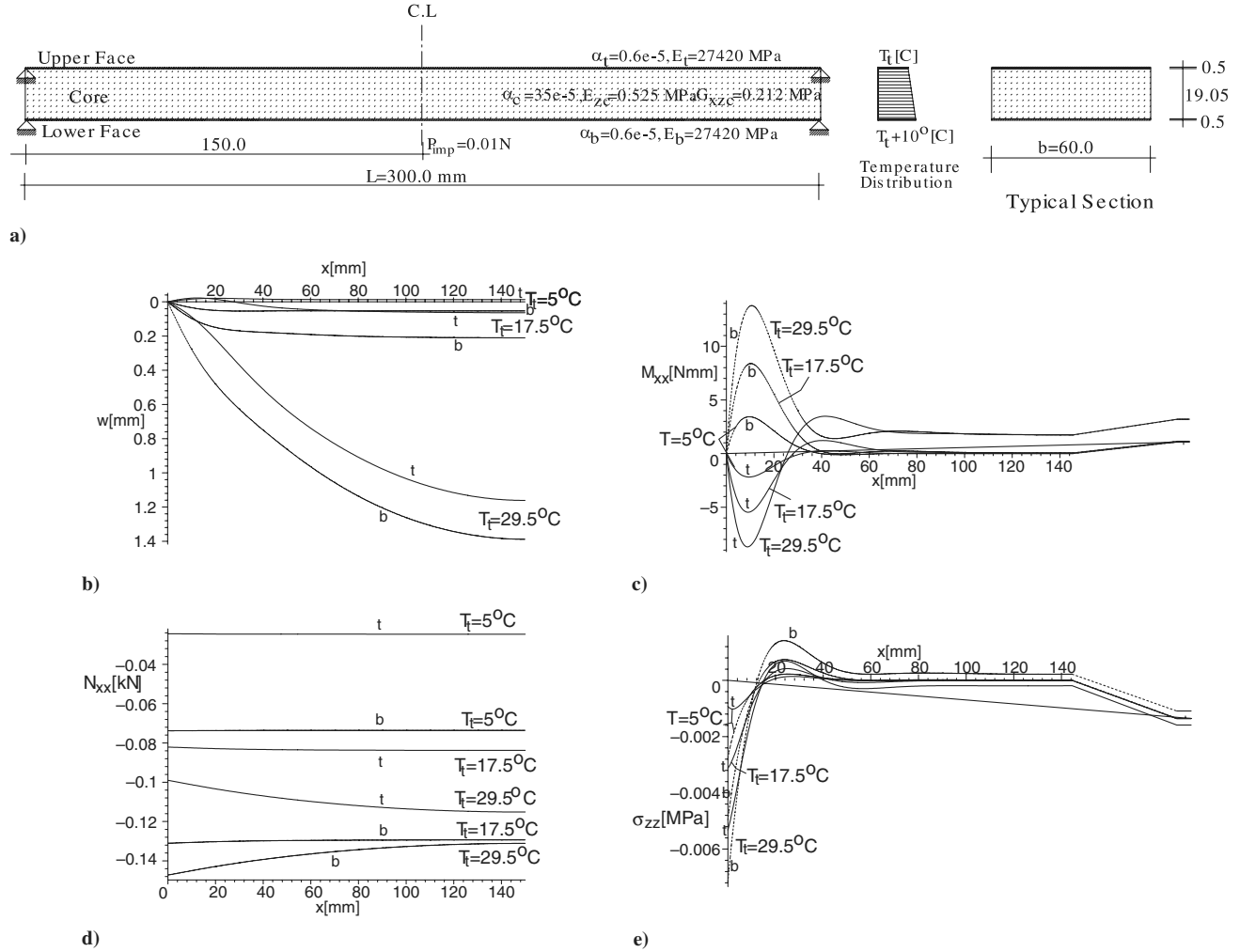

Fig. 9 Geometry and results along half-span of a sandwich panel with a gradient temperature distribution at $T_t = 5°C$ (linear), $T_t = 17.5°C$ (at buckling) and $T_t = 29.5°C$: a) geometry and mechanical properties, b) vertical displacements, c) bending moments, d) in-plane stress resultants, and e) interfacial vertical normal stresses at interfaces; *t* upper-face interface (solid line) and *b* lower-face interface (dashed line).

comparison with the vertical displacements of the wrinkling-type buckling (see Fig. 4a). The values of the extreme displacements for the different α_C values are of the same order of magnitude, and they increase as the α_C increases. Notice that for the case with the larger α_C value, the displacements of the upper face are the smallest, as a result of the large vertical expansion of the core that causes the upper face to move upward. The FE results by ANSYS for the case with the larger CTE reveal a very similar displacement layout, which almost coincides throughout the panel except for the midspan vicinity, in which the ANSYS displacements have a similar pattern but with slightly larger values. The differences between the results of the two different approaches are due to the large-displacement kinematic relations used by ANSYS, compared with the large displacement and moderate rotations used here. The bending moments for the faces are identical in values but of opposite signs (see Fig. 7b), and they reach their largest values in the vicinity of the support. Again, the peak values increases as α_C increases. The in-plane stress resultants are compressive (see Fig. 7c), and they vary along the span, as a result of the existence of shear stresses in the core. Moreover, the in-plane stress resultants exceed the critical load of $N_{o,\mathrm{gl}} = -0.126$ kN of the linearized solution. The vertical normal interfacial stresses at the upper- and lower-face–core interfaces are almost identical, although the panel moves downward. In the case of $\alpha_C = 0$, they are almost zero, whereas they reach higher values in the vicinity of the supports as α_C is increased. In general, when a panel moves downward as a result of bending or buckling, the interfacial stresses at the various interfaces are of different signs: one is in tension and the other one is in compression. Here, the behavior is different, due to the vertical thermal expansion of the core that causes the formation of compressive vertical normal interfacial stresses before the global bending displacements.

The equilibrium curves of temperature vs extreme structural quantities for the three α_C values for the case of global buckling appear in Fig. 8. In the case of $\alpha_C = 0$, a significant change in the shape of the curves is observed in the vicinity of and below the critical temperature of the linearized approach of $T_{\mathrm{cr,gl}} = 25.59°\mathrm{C}$. The curves for vertical displacements at the two face sheets appear in Fig. 8a. Here, all curves exhibit a change in the pattern of the curves, which reflects the existence of a bifurcation point, although below the critical temperature. A comparison with FE results by ANSYS for the case with the larger CTE reveals similar trends, with some discrepancies at lower temperatures that decrease as the temperature is increased. The differences are due to the kinematic relations of large displacements and large rotations used by the FE analysis, compared with the kinematic relations of large deformations with moderate rotations used by the proposed model. Notice that in all three cases, as well as with ANSYS, the postbuckling curve is of a stable type (plate type), which means that any increase in the displacement is caused by an increase in the temperature. A similar trend is observed for the maximum bending moments of the first two α_C values, whereas for the largest α_C, a general nonlinear behavior is detected (see Fig. 8b). The interfacial vertical normal stresses exhibit a postbuckling behavior only in the case of $\alpha_C = 0$, whereas a general nonlinear behavior is seen for nonzero α_C values (see Fig. 8d). Also, the ANSYS results here compare very well with those of the proposed analysis.

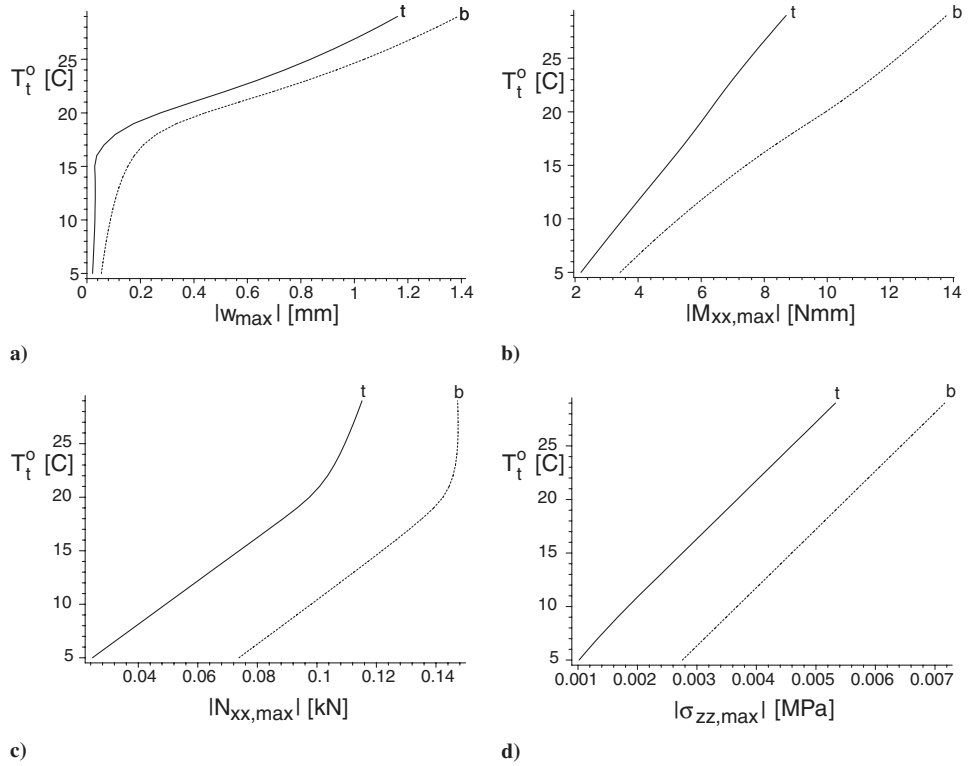

Fig. 10 Nonlinear response curves, temperature vs extreme values with a thermal gradient: a) vertical displacements, b) bending moments, c) in-plane compressive stress resultants, and d) interfacial vertical normal stresses at interfaces; *t* upper-face interface (solid line) and *b* lower-face interface (dashed line).

The equilibrium curves of the in-plane compressive stress resultants in the two face sheets appear in Fig. 8c, and they were determined using the imperfection loads that appear in Fig. 6a. For all three α_C cases, a significant change is observed in the vicinity of the critical temperature. The resultants in the various face sheets are not identical, as a result of the overall bending that cause additional compression in the upper-face sheet and tension in the lower-face sheet. Notice that here, the compressive resultants reach values that are larger than the critical compressive resultant $N_{o,\mathrm{gl}} = -0.126$ kN of the linearized solution, compared with the wrinkling case. The results of the wrinkling and the global-buckling-type analyses indicate that the critical buckling mode is the global one, and it occurs at a rather low temperature of about 25°C.

The second case study presents the nonlinear response of a sandwich panel when subjected to thermal field, which consists of a thermal gradient distribution through the depth of the core and uniform distribution through the length of the panel. For the geometry and mechanical properties, see Fig. 9a. The gradient distribution assumes a uniform distribution at the upper-face sheet, a gradient of 10°C in the core, and a uniform distribution in the lower-face sheet (see the temperature distribution in Fig. 9a).

The results along the half-span of the sandwich panel appear in Fig. 9a at three temperature levels of the upper-face sheet: 5°C, in the vicinity of the critical temperature of 17.5°C, and deep into the postbuckling range at 25°C. The various displacement patterns appear in Fig. 9b. Their magnitudes increase as the temperature level is raised. The displacements at the lower temperature mainly reflect the deformation caused by the expansion of the core at low temperature levels. Similar trends are observed for the bending moments that reach their extreme values in the vicinity of the support (see Fig. 9c). The in-plane compressive resultants (see Fig. 9d) are uniform at the lower temperature levels and increase and change into nonlinear behavior as the temperature is raised as a result of the formation of shear stresses in the core. Finally, the interfacial vertical normal stresses follow the same trends as those of the bending moments, and they reach their maximum values in the vicinity of the support (see Fig. 9e).

The equilibrium curves for this case appear in Fig. 10 and the imperfection loads used here are due to the gradient of temperatures between the face sheets. A significant change in the curves that indicates the occurrence of buckling is seen for the maximum displacements and the in-plane compressive stress resultants in the vicinity of a temperature of 17°C of the upper-face sheet. This critical temperature is lower than those obtained for global buckling of the previous case (see Fig. 10a vs Fig. 8a and Fig. 10c vs Fig. 8c). The curves of the displacements of the face sheets appear in Fig. 10a and reflect a stable postbuckling behavior. Notice that the lower-face sheets exhibit larger displacements than the upper-face sheets, which indicates a nonlinear response as a result of the vertical expansion of the core. The bending moments and the interfacial stresses exhibit a general nonlinear response (see Figs. 10b and 10d). The curves of the compressive stress resultants appear in Fig. 10c, and they reflect a bifurcation point. In the postbuckling range, the compressive resultants in the lower-face sheet that buckles first reaches a value of 0.145 kN, which is larger than the critical resultant predicted by the linearized model of 0.126 kN, and remains unchanged and even decreases as the temperature is raised. In the lower-face sheet, the compressive stress resultants increase as the temperature increases.

Conclusions

The nonlinear thermal behavior, along with buckling and postbuckling, of a sandwich panel with a soft core and immovable supports (in-plane restraints) is presented. The mathematical formulation is based on a variational approach and the high-order sandwich-panel-theory approach. The analysis considers the thermal strains of the core in the vertical direction and the effects of the vertical flexibility of the core. The nonlinear governing equations are linearized using the perturbation approach, thus yielding the equations for the prebuckling and the buckling stages. In general, the equations of the prebuckling state are nonlinear, and they do not describe a membrane state. However, when the thermal expansion or contraction of the core in the vertical direction is ignored, the linearized equations exhibit a membrane state at the prebuckling

stage, and a closed-form analytical solution exists in the case of a uniform thermal field along the sandwich-panel length. The critical temperatures and their modes are determined in the case of a simply supported sandwich panel with movable supports at the buckling state. Two types of buckling are observed: local buckling or wrinkling, in which the two face sheets move opposite to each other, and global buckling, in which the two face sheets move in the same direction.

The postbuckling response is determined through the solution of the full nonlinear analysis, and the characteristic solution features are demonstrated for some typical cases with wrinkling and global types of buckling and for the case of a sandwich panel subjected to a gradient thermal distribution. The nonlinear response yields critical temperatures in the vicinity of the results obtained using the simplified linearized models. In all cases, the postbuckling response is of a stable type (plate type), in which any increase in the displacement is associated with an increase of the temperature.

The effects of the coefficient of thermal expansion of the core are studied, and the results are compared with the results obtained using the simplified linearized model. The nonlinear results for the largest CTE compare very well with FE results of ANSYS for the wrinkling and the overall buckling cases. The study reveals that in the case of wrinkling buckling with $\alpha_C = 0$, the sandwich panel exhibits buckling behavior at a temperature that equals the result of the linearized model. However, when the vertical thermal strains of the core are considered, the response is generally nonlinear, without a bifurcation point at the critical temperature $T_{\mathrm{cr,wr}}$, whereas the in-plane compressive stress resultants are smaller than those defined in the linearized approach. Thus, an approach that defines the structural capacity of a heated sandwich panel using the elastic foundation approach is, in general, physically inconsistent and incorrect.

In the case of global buckling, the response is that of a bifurcation with a stable postbuckling curve, whether the vertical thermal strains of the core are included in the analysis or not. The nonlinear critical temperature is lower than that predicted by the linearized solution $T_{\mathrm{cr,gl}}$. The case with gradient thermal fields follows the same trends of global buckling, but with a lower critical temperature.

The full nonlinear model provides a rigorous consistent approach that fulfills all constraints imposed on the sandwich panel, especially when the compressive stress resultants are a result of in-plane restrains (immovable supports). The linearized approach contradicts the real support conditions and may serve only as an initial trial solution for the nonlinear analysis.

Finally, a typical uniformly heated sandwich panel with a soft core generally exhibits a nonlinear response with and without a bifurcation-point buckling phenomenon and a stable postbuckling behavior.

Acknowledgments

The work presented was conducted during the period of a visiting professorship of the first author with the Institute of Mechanical Engineering at Aalborg University, sponsored by the U.S. Navy, Office of Naval Research (ONR), grant/award N00014-04-1-0112: "Localized Effects in Advanced Lightweight Sandwich Structures." The ONR program manager was Yapa Rajapakse. The financial support received is gratefully acknowledged. The ANSYS runs were conducted by O. Rabinovitch. His assistance is gratefully acknowledged.

References

[1] Allen, H. G., *Analysis and Design of Structural Sandwich Panels*, Pergamon, London, 1969.

[2] Plantema, F. J., *Sandwich Construction*, Wiley, New York, 1966.

[3] Zenkert, D., *An Introduction to Sandwich Construction*, Chameleon, London, 1995.

[4] Vinson, J. R., *The Behavior of Sandwich Structures of Isotropic and Composite Materials*, Technomic, Lancaster, PA, 1999.

[5] Bulson, P. S., *The Stability of Flat Plates*, Chatto and Windus, London, 1970.

[6] Brush, D. O., and Almroth, B. O., *Buckling of Bars, Plates, and Shells*, McGraw–Hill, New York, 1975.

[7] Vinson, J. R., and Sierakowski, R. L., *The Behavior of Structures Composed of Composite Materials*, Martinus Nijhoff, Dordrecht, The Netherlands, 1986.

[8] Mindlin, R. D., "Influence of Transverse Shear Deformation on the Bending of Classical Plates," *Journal of Applied Mechanics*, Vol. 18, 1951, pp. 31–38.

[9] Reddy, J. N., *Energy and Variational Methods in Applied Mechanics*, Wiley, New York, 1984.

[10] Ko, W. L., "Mechanical and Thermal Buckling Analysis of Rectangular Sandwich Panels Under Different Edge Conditions," NASA TM-4585, 1994.

[11] Kant, T., and Babu, C. S., "Thermal Buckling Analysis of Skew Fiber-Reinforced Composite and Sandwich Plates Using Shear Deformable Finite Element," *Composite Structures*, Vol. 49, No. 1, 2000, pp. 77–85.
doi:10.1016/S0263-8223(99)00127-0

[12] Najafizadeh, M. M., and Heydari, H. R., "Thermal Buckling of Functionally Graded Circular Plates Based on Higher-Order Shear Deformation Plate Theory," *European Journal of Mechanics, A/Solids*, Vol. 23, No. 6, 2004, pp. 1085–1100.
doi:10.1016/j.euromechsol.2004.08.004

[13] Lanhe, W., "Thermal Buckling of Simply Supported Moderately Thick Rectangular FGM Plate," *Composite Structures*, Vol. 64, 2004, pp. 211–218.
doi:10.1016/j.compstruct.2003.08.004

[14] Shiau, L. C., and Kuo, S. Y., "Thermal Postbuckling Behavior of Composite Sandwich Plates," *Journal of Engineering Mechanics*, Vol. 130, No. 10, 2004, pp. 1160–1167.
doi:10.1061/(ASCE)0733-9399(2004)130:10(1160)

[15] Matsunaga, H., "Thermal Buckling of Cross-Ply Laminated Composite and Sandwich Plates According to a Global High-Order Deformation Theory," *Composite Structures*, Vol. 68, No. 4, 2005, pp. 439–454.

[16] Thomsen, O. T., "Theoretical and Experimental Investigation of Local Bending Effects in Sandwich Plates," *Composite Structures*, Vol. 30, No. 1, 1995, pp. 85–101.
doi:10.1016/0263-8223(94)00029-8

[17] Ko, W. L., and Jackson, R. H., "Thermal Behavior of a Titanium Honeycomb-Core Sandwich Panel," NASA TM-101732, 1991.

[18] Rao, V. G., and Raju, K. K., "Thermal Postbuckling of Uniform Columns on Elastic Foundation-Intuitive Solution," *Journal of Engineering Mechanics*, Vol. 129, No. 11, 2003, pp. 1351–1354.
doi:10.1061/(ASCE)0733-9399(2003)129:11(1351)

[19] Birman, V., "Thermally Induced Bending and Wrinkling in Large Aspect Ratio Sandwich Panels," *Composites, Part A: Applied Science and Manufacturing*, Vol. 36, No. 10, Oct. 2005, pp. 1412–1420.
doi:10.1016/j.compositesa.2004.11.013

[20] Birman, V., Kardomateas, G. A., Simitses, G. J., and Liu, L., "Response of a Sandwich Panel Subject to Fire or Elevated Temperature on One of the Surfaces," *Composites, Part A: Applied Science and Manufacturing*, Vol. 37, No. 7, 2006, pp. 981–988.
doi:10.1016/j.compositesa.2005.03.014

[21] Liu, L., Kardomateas, G. A., Birman, V., Holmses, J. W., and Simitses, G. J., "Thermal Buckling of a Heat-Exposed, Axially Restrained Composite Column," *Composites, Part A: Applied Science and Manufacturing*, Vol. 37, No. 7, 2006, pp. 972–980.
doi:10.1016/j.compositesa.2005.04.006

[22] Frostig, Y., "Hygothermal (Environmental) Effects in High-Order Bending of Sandwich Beams with a Flexible Core and a Discontinuous Skin," *Composite Structures*, Vol. 37, No. 2, 1997, pp. 205–221.
doi:10.1016/S0263-8223(97)80013-X

[23] Frostig, Y., and Baruch, M., "Buckling of Simply Supported Sandwich Beams with Transversely Flexible Core a High Order Theory," *Journal of Engineering Mechanics*, Vol. 119, No. 3, 1993, pp. 476–495.
doi:10.1061/(ASCE)0733-9399(1993)119:3(476)

[24] Frostig, Y., "Buckling of Sandwich Panels with a Transversely Flexible Core-High-Order Theory," *International Journal of Solids and Structures*, Vol. 35, Nos. 3–4, 1998, pp. 183–204.
doi:10.1016/S0020-7683(97)00078-4

[25] Sokolinsky, V., and Frostig, Y., "Branching Behavior in the Non-Linear Response of Sandwich Panels with a Transversely Flexible Core," *International Journal of Solids and Structures*, Vol. 37, 2000, pp. 5745–5772.
doi:10.1016/S0020-7683(99)00232-2

[26] Frostig, Y., and Thomsen, O. T., Sheinman, I., "On the Non-Linear High-Order Theory of Unidirectional Sandwich Panels with a Transversely Flexible Core," *International Journal of Solids and Structures*, Vol. 42, Nos. 5–6, Mar. 2005, pp. 1443–1463.
doi:10.1016/j.ijsolstr.2004.08.015

[27] Simitses, G. J., *An Introduction to the Elastic Stability of Structures*, Prentice–Hall, Upper Saddle River, NJ, 1976.
[28] Frostig, Y., and Thomsen, O. T., "Localized Effects in the Non-Linear Behavior of Sandwich Panels with a Transversely Flexible Core," *Journal of Sandwich Structures and Materials*, Vol. 7, No. 1, Jan. 2005, pp. 53–75. doi:10.1177/1099636205046207
[29] Stoer, J., and Bulirsch, R., *Introduction to Numerical Analysis*, Springer, New York, 1980.
[30] Keller, H. B., *Numerical Methods for Two-Point Boundary Value Problems*, Dover, New York, 1992.
[31] ANSYS, Software Package, Ver. 8.1, ANSYS, Inc., Canonsburg, PA, 2006.

A. Roy
Associate Editor